

**CELL-BASED DRUG DEVELOPMENT,
SCREENING, AND TOXICOLOGY**

Systemic multipotent adult progenitor cells protect the cerebellum after asphyxia in fetal sheep

Ruth Gussenhoven^{1,2} | Daan R.M.G. Ophelders^{1,3} | Jeroen Dudink⁴ | Kay Pieterman⁵ |
 Martin Lammens⁶ | Robert W. Mays⁷ | Luc J. Zimmermann^{1,3} |
 Boris W. Kramer^{1,2,3} | Tim G.A.M. Wolfs^{1,3}  | Reint K. Jellema¹ 

¹Department of Pediatrics, Maastricht University Medical Centre, Maastricht, The Netherlands

²School of Mental Health and Neuroscience, Maastricht University, Maastricht, The Netherlands

³School of Oncology and Developmental Biology, Maastricht University, Maastricht, The Netherlands

⁴Department of Neonatology, Wilhelmina Children's Hospital and Brain Centre Rudolf Magnus, University Medical Centre Utrecht, Utrecht, The Netherlands

⁵Biomedical Imaging Group Rotterdam, Department of Radiology and Medical Informatics, Erasmus Medical Centre, Rotterdam, The Netherlands

⁶Department of Pathology, Antwerp University Hospital and University of Antwerp, Edegem, Belgium

⁷Regenerative Medicine, Athersys, Inc., Cleveland, Ohio

Correspondence

Reint K. Jellema, MD, PhD, Department of Pediatrics, Maastricht University Medical Center, PO Box 5800, 6202 AZ Maastricht, The Netherlands.
 Email: reint.jellema@maastrichtuniversity.nl

Funding information

Athersys, Inc.

Abstract

Involvement of the cerebellum in the pathophysiology of hypoxic-ischemic encephalopathy (HIE) in preterm infants is increasingly recognized. We aimed to assess the neuroprotective potential of intravenously administered multipotent adult progenitor cells (MAPCs) in the preterm cerebellum. Instrumented preterm ovine fetuses were subjected to transient global hypoxia-ischemia (HI) by 25 minutes of umbilical cord occlusion at 0.7 of gestation. After reperfusion, two doses of MAPCs were administered intravenously. MAPCs are a plastic adherent bone-marrow-derived population of adult progenitor cells with neuroprotective potency in experimental and clinical studies. Global HI caused marked cortical injury in the cerebellum, histologically indicated by disruption of cortical strata, impeded Purkinje cell development, and decreased dendritic arborization. Furthermore, global HI induced histopathological microgliosis, hypomyelination, and disruption of white matter organization. MAPC treatment significantly prevented cortical injury and region-specifically attenuated white matter injury in the cerebellum following global HI. Diffusion tensor imaging (DTI) detected HI-induced injury and MAPC neuroprotection in the preterm cerebellum. This study has demonstrated in a preclinical large animal model that early systemic MAPC therapy improved structural injury of the preterm cerebellum following global HI. Microstructural improvement was detectable with DTI. These findings support the potential of MAPC therapy for the treatment of HIE and the added clinical value of DTI for the detection of cerebellar injury and the evaluation of cell-based therapy.

KEYWORDS

asphyxia, cerebellum, hypoxic-ischemic encephalopathy, MAPC, stem cells

Ruth Gussenhoven and Daan R. M. G. Ophelders contributed equally to this study.

This is an open access article under the terms of the Creative Commons Attribution-NonCommercial-NoDerivs License, which permits use and distribution in any medium, provided the original work is properly cited, the use is non-commercial and no modifications or adaptations are made.

© 2020 The Authors. STEM CELLS TRANSLATIONAL MEDICINE published by Wiley Periodicals LLC on behalf of AlphaMed Press.

1 | INTRODUCTION

Hypoxic-ischemic encephalopathy (HIE) is an important cause of mortality and morbidity in preterm neonates.¹ Global HIE in preterm infants affects individual brain regions differently.^{1,2} HIE was recognized primarily as a white matter disease of the cerebrum, leaving cerebellar involvement underappreciated in the clinical setting.² However, previous findings demonstrate that cerebellar injury plays an important role in the high prevalence of nonmotor deficits (ie, cognition, learning, and behavior) in survivors of prematurity.^{3,4}

During the third trimester of pregnancy, the cerebellum exhibits a rapid increase in growth and development.² Any disturbance of cerebellar growth, for example, by hypoxia-ischemia or inflammation, may lead to irreversible aberrations of the cerebellar integrity.^{2,5} Moreover, cerebellar lesions in the developing brain can cause or aggravate contra-lateral supratentorial deficits (cerebellocerebral diaschisis).²

Until recently, acute cerebellar injuries were rarely detected with conventional clinical neuroimaging, such as T1- and T2-weighted magnetic resonance imaging (MRI).⁶ Clinical imaging studies using new advanced MRI modalities, including diffusion tensor imaging (DTI), however, showed that cerebellar injury in premature survivors with neonatal encephalopathy is common and associated with adverse clinical outcome.⁷ Moreover, disturbed cerebellar development in prematurely born children can still be detected at school age/adolescence with advanced neuroimaging.⁸

Therefore, protection of the cerebellum following preterm birth and/or HI is clinically highly relevant and cell-based therapy has proven to be a promising treatment to improve neurodevelopmental outcomes in preterm infants.⁹ We have previously shown that intravenous administration of mesenchymal stem cells and multipotent adult progenitor cells (MAPCs) protect cerebral structure and function in a fetal sheep model of HIE.^{10,11} In this model of preterm brain injury, we demonstrated that the injurious effects of global hypoxia-ischemia and therapeutic effects of intravenous stem cell therapy could be readily detected in the cerebral white matter using DTI.¹⁰

The primary aim of this study was therefore to assess the neuroprotective potential of MAPCs in the cerebellum following global hypoxia-ischemia (HI). We hypothesized that MAPC therapy would reduce structural injury in the preterm cerebellum following global HI. To test this hypothesis, 0.7 gestation instrumented fetal sheep were exposed to global hypoxia-ischemia by umbilical cord occlusion (UCO) and subsequently treated with intravenously delivered MAPCs. Cerebellar injury was assessed by histopathology and diffusion weighted MRI.

2 | MATERIALS AND METHODS

2.1 | Study approval

All animal procedures were performed in accordance with the guidelines and approval of the institutional Animal Ethics Research committee of Maastricht University, The Netherlands.

Significance statement

Cerebellar injury after asphyxia was reduced with systemic multipotent adult progenitor cells (MAPCs) therapy. These findings in the cerebellum essentially extended the authors' previous experimental work showing that MAPCs induced structural and functional neuroprotection after asphyxia in the ovine cerebrum. MAPCs are a clinical-grade product with extensively proven safety. A recent clinical trial in adult stroke patients showed that MAPCs improved functional outcomes after 1-year follow-up. This study in a relevant large animal model with clinical-grade stem cells greatly improves the potential for translation into neonatal medicine.

2.2 | Multipotent adult progenitor cells

MAPCs are a plastic adherent bone-marrow-derived population of adult progenitor cells with long-term culture expansion and potency.^{12,13} MultiStem, the clinical grade MAPC product, is currently being tested for neuroprotection in an international phase III trial of adult stroke (ClinicalTrials.gov NCT03545607).¹⁴ Differentiation capacity, functional characteristics, and genomic and epigenetic stability of the MAPCs were confirmed as previously described.^{12,13} MAPCs were expanded under good manufacturing practice as previously described¹⁵ and stored in liquid nitrogen. Before administration, the MAPCs were thawed and washed twice and suspended in phosphate buffered saline (PBS) at a concentration of 10×10^6 cells/mL. The fetuses randomized to MAPC treatment received two intravenously delivered doses of 10×10^6 cells in 1 mL PBS via the right brachial vein. The first dose was administered 1 hour after reperfusion. The second dose was administered on day 4 after reperfusion.

2.3 | Experimental design

Fetuses of time-mated Texel ewes were instrumented as previously described.¹⁰ The outcome of the cerebrum of these animals has been previously reported.¹¹ We assessed the cerebellum of 23 ($n = 26$) singleton fetuses (both sexes), which had been randomly assigned to one of the four following experimental groups: (a) sham UCO, saline treatment (sham-SAL; $n = 8$), (b) sham UCO, MAPC treatment (sham-MAPC; $n = 4$), (c) UCO, saline treatment (HI-SAL or HI; $n = 7$), and (d) UCO, MAPC treatment (HI-MAPC; $n = 7$). Power analysis indicated that with a sample size of $n = 5$ in the HI-MAPC group significant treatment effects could be detected in the cerebellum, which was based on previous reported MAPC-mediated white matter protection in the cerebrum.¹¹ Previous clinical¹⁴ and experimental^{11,16-18} work has extensively shown safety of MAPCs under control conditions. Therefore, a smaller sham-MAPC group of $n = 4$ was considered

acceptable to exclude MAPC-induced changes in the cerebellum under sham conditions.

Fetal instrumentation was performed at 102 days of gestation (experimental day -4). At 106 days of gestation (experimental day 0) fetuses were subjected to 25 minutes of UCO or sham conditions. At the time of UCO, brain maturation is broadly equivalent to 30 weeks of human gestation which coincides with the high-risk window of brain injury in preterm infants.¹⁹ The dynamics of physiological parameters during UCO were previously reported.¹¹ Blood pressure, heart rate, pH, pCO₂, and pO₂ at different time points are shown in Table S1. Fetuses received two doses of MAPCs or an equal volume of the saline vehicle (1 hour and 4 days following UCO). Randomization, (sham) UCO and tissue sampling was performed by investigators who were blinded for treatment allocation.

2.4 | Brain sampling

After a reperfusion period of 7 days, animals were sacrificed at 113 days of gestation with intravenous pentobarbitone (200 mg/kg). Brains were collected and the right hemisphere was submersion fixated in 4% paraformaldehyde (PFA) at 4°C for 3 months.

2.5 | Magnetic resonance imaging

To wash out the PFA, 48 hours prior to MRI imaging the right hemisphere was washed with PBS and stored in PBS containing 1% sodium azide. DTI images were acquired using an echo planar imaging (EPI) sequence with diffusion gradients ($b = 4000$ seconds/mm²) applied in 66 noncollinear directions and 6 B0 measurements. An average of 60 slices was recorded within 36 minutes using a repetition time (TR) = 500 ms and echo time (TE) = 75 ms. Isovolumetric voxel size was 0.5 mm³. The field of view (FOV) was 30 × 60 × 60 mm and scan matrix size 60 × 120 × 60 mm.

Diffusion weighted images were processed using ExploreDTI version 4.8.6 running in Matlab (R2015, The MathWorks, Inc., Natick, Massachusetts).²⁰ To optimize image quality, all data sets were corrected for motion, EPI-induced distortions, and Eddy currents.^{20,21} Diffusion tensors were calculated robustly using the REKINDLE approach to exclude motion-induced outliers prior to tensor estimation.²² For each data set, color-coded fractional anisotropy (FA) maps were spatially aligned with the T2 image, and visualized as a semitransparent overlay on the T2 maps. This visualization approach improved localization of the desired anatomical regions of interest. After region of interest (ROI) placement in the cerebellum (white matter and cortex), FA values were obtained for each ROI in Explore DTI. Manual delineation of ROIs was performed by a neonatologist with expertise in DTI analysis who was blinded for the treatment allocation.

2.6 | Histology and immunohistochemistry

The right hemisphere of the cerebellum was embedded in paraffin and serial sagittal sections (4 μm) were cut with a Leica RM2235 microtome (Leica, Rijswijk, The Netherlands).²³ At the intersection of the cerebellar peduncles, Nissl and Luxol Fast Blue (LFB) stainings were performed for morphological and anatomical analysis. Immunohistochemical analysis was performed on three sections per animal (every 10th consecutive section). Adjacent sections were stained with an anti-ionized calcium binding adaptor molecule 1 (IBA-1) antibody (019-19 741, Wako Pure Chemical Industries) for microglia, a glial fibrillary acidic protein (GFAP) antibody (ZO334, Dako) for astroglia, a myelin basic protein (MBP) antibody (MAB386, Millipore) for mature oligodendrocytes and myelin, a calbindin antibody (CB-38a, Swant) for Purkinje cells (PC), and a cleaved caspase-3 antibody (#9664, Cell signaling) for apoptotic cell death.

Endogenous peroxidase activity was inactivated with 0.3% H₂O₂ treatment. Antigen retrieval was performed by microwave boiling of tissue sections in citrate buffer (pH 6.0).²³ Nonspecific binding was blocked by incubation with bovine, goat, or donkey serum in PBS. Sections were incubated overnight at 4°C with the diluted primary antibody (IBA-1, GFAP, MBP & Caspase-3 1:1000; calbindin 1:6000). The following day sections were incubated with the specific secondary antibody and staining was enhanced with a Vectastain ABC peroxidase Elite kit (Vector Laboratories, Inc., Burlingame, California) and (nickel) 3,3'-diaminobenzidine staining.

2.7 | Qualitative analysis

Nissl stained sections were analyzed by a neuropathologist with expertise in the field of neonatal brain injuries and two independent researchers who were blinded for the experimental setup. Sections were assessed for structural and inflammatory changes including the presence of gliosis, hemorrhages, and structural damage including cyst formation. LFB sections were evaluated for myelin structure and myelin abnormalities.

2.8 | Quantitative analysis of Nissl staining

The thickness of cerebellar strata was measured on Nissl stained sections. The molecular layer (ML) and external granular layer (EGL) thickness were determined in ImageJ 1.49v (U. S. National Institutes of Health, Bethesda, Maryland) using ×20 images of lobule I-X from Nissl stained cerebellar sections. The thickness of the ML was defined as the distance between the top of the purkinje cell (PC) soma and the internal border of the EGL. EGL thickness was determined relative to the ML. Measurements were performed in duplicate by two independent researchers on 20 images per animal. One image was taken of the crest and one of the insert of each lobule (lobule I-X) (Figure 1), resulting in 20 images per animal.

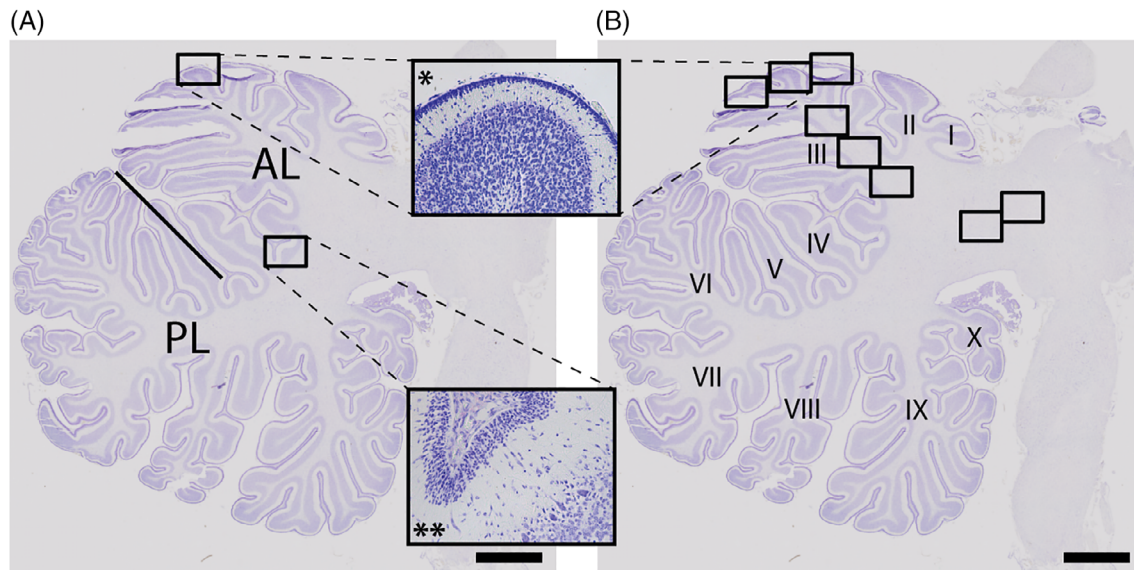


FIGURE 1 Overview of quantitative analysis. A,B, Immunohistochemical Nissl staining depicting regions of interest in the cerebellum. A, Thickness of the external granular layer and molecular layer was measured in the crest (*) and inserts (**) of the anterior lobe and the posterior lobe of the cerebellum. B, Immunohistochemical stainings were analyzed in lobe III and in lobe IX and in the cerebellar peduncles. The black squares indicate the regions of interest in cerebellar white matter, cerebellar cortex, and the peduncles. * = crest of the lobule; ** = inset of lobule. Scale bar = 5 mm. AL, anterior lobe; PL, posterior lobe

2.9 | Quantitative analysis of immunohistochemical stained sections

Immunohistochemical stainings were analyzed using a light microscope (Leica DM2000) equipped with Leica QWin Pro version 3.4.0 software (Leica Microsystems, Mannheim, Germany). Inflammatory changes were assessed by IBA-1 immunoreactivity (IR) and white matter alterations were assessed by MBP IR in the anterior cerebellum (lobule III) and posterior cerebellum (lobule IX) (Figure 1). ROIs were both the white matter and cortex of the cerebellum; as illustrated in Figure 1 the cortical ROI comprised all three cortical layers, that is, internal granular layer (IGL), ML, and EGL, whereas the white matter was marked from the beginning of the lobe till the boundary of the IGL. Area fractions were determined using a standard threshold to detect positive staining with Leica QWin Pro V 3.5.1 software (Leica, Rijswijk, The Netherlands). In the same regions, caspase positive cells were counted and expressed as positive cells/mm².

PC density was quantified by counting all cell somas positive for calbindin that intersect with a horizontal line of known length and then dividing the number of cells by the length of the line. Counting was performed in lobule III and IX in four random fields of views per lobule.

The areal densities of GFAP⁺ cells and in particular GFAP⁺ Bergmann glia that are only located in the ML were determined by measuring area fractions of GFAP IR in the cerebellar white matter and IGL and ML of the cerebellar cortex using Leica QWin Pro V 3.5.1 software (Leica, Rijswijk, The Netherlands). In addition to area fractions, the linear density of the Bergmann glial fibers (GFAP⁺ fibers) in the ML was determined using ImageJ. Perpendicular to the Bergmann

glial fibers a horizontal line was drawn and fibers that intersected this line were counted in three random fields of view in lobule III and three in lobule IX (six fields of view per animal). Linear density was calculated by dividing the number of intersecting fibers by the length of the line and displayed in intersections/mm.

2.10 | Statistical analysis

Summary statistics of all outcome variables are shown as means with SE of the mean (SEM). Groups' comparisons of all outcome parameters were drawn with analysis of variance or with random intercept models in case of repeated measurements per animal (eg, different sections per brain). HI (sham vs HI) and treatment (saline vs MAPC) were the fixed effects. For random intercept models, animals constituted additionally the random effect. A false discovery rate (FDR) of 5% was used for multiple testing corrections. Groups' differences with FDR corrected $P < .05$ were considered statistically significant. Statistical analysis was performed with IBM SPSS Statistics Version 22.0 (IBM Corp., Armonk, New York; SPSS, RRID: SCR_002865) and GraphPad Prism software (version v5.0; GraphPad Software, Inc., La Jolla, California).

3 | RESULTS

Structural and functional benefits of MAPC in the cerebrum after global HI have been previously reported.¹¹ Reproducibility of the animal model was confirmed by nonsignificant differences in bradycardia,

hypotension, hypoxia, and combined acidosis between the HI-SAL and HI-MAPC groups (Table S1). One animal in the HI-MAPC group was excluded from analysis because of maternal postoperative complications necessitating early delivery (day 3 post-UCO) of the fetus before the end of the experiment (day 7 post-UCO). In the cerebellum, no significant differences in histopathological and neuroimaging outcome parameters were found between the sham-SAL and sham-MAPC group which is consistent with previous experimental studies.^{11,16,18} For readability, only a representative histological image of the sham-SAL group was shown (Figures 2, 4, and 5).

3.1 | MAPC therapy prevented histopathological alterations in the cerebellar cortex after global HI

Global HI significantly induced a decrease of the ML thickness (sham-SAL vs HI-SAL $P < .001$) and—to a lesser extent—a significant decrease in EGL thickness (sham-SAL vs HI-SAL $P = .043$). This resulted in a significant increase of the EGL/ML-ratio (sham-SAL vs HI-SAL $P = .032$) (Figure 2). Following HI, cortical layers were

morphologically less defined and cellular density within the EGL and ML was increased following HI compared to control animals (Figure 2).

Purkinje cells (PCs) were analyzed based on cell number and morphology by means of Nissl and calbindin staining. Nissl staining showed that global HI reduced the number of morphologically normal PCs, increased empty spaces or gaps within the PC layer, and increased the number of pyknotic PCs (Figure 2). Pyknotic PCs showed shrunken nuclei with chromatin condensation and reduced or bright pink, acidophilic cytoplasm (Figure 2D, inset). Moreover, there were more PCs present in the IGL and cerebellar white matter following HI compared to controls, indicating more ectopic PCs (data not shown).

Global HI-induced loss of PCs was confirmed by a significant (sham-SAL vs HI-SAL $P < .001$) decrease of calbindin⁺ cells following HI (Figure 2). In addition, dendritic arborization of calbindin⁺ cells was reduced following HI compared to controls indicating altered Purkinje cell development or injury (Figure 2). Interestingly, the reduction of dendritic arborization in the cerebellar cortex was more pronounced in the anterior lobes compared to the posterior lobes of the

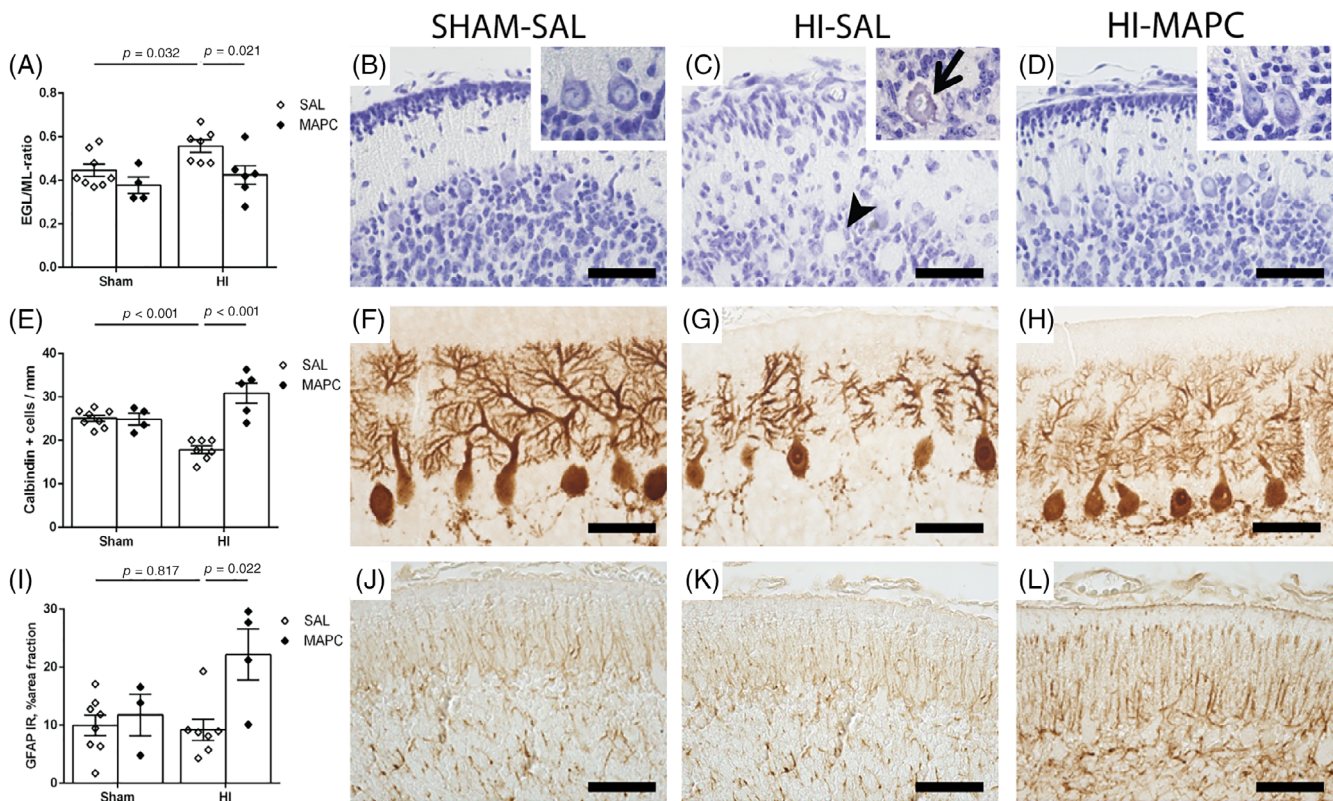


FIGURE 2 MAPC treatment protected HI-induced cerebellar cortical alterations. Graphical presentation of (A) EGL/ML-ratio, (E) calbindin⁺ cells, and (I) GFAP linear density in the cerebellar cortex. Means ± SEM and levels of significance are depicted. Immunohistochemical (B-D), Nissl (F-H) calbindin, and (J-L) GFAP staining in the cerebellar cortex at ×400 magnification. Global HI increased the EGL/ML-ratio and decreased the number of calbindin⁺ cells in the preterm cerebellum. Furthermore, global HI increased the number of pyknotic cells (arrow in insert of panel C), caused more “gaps” within the PC layer (arrowhead in panel C), and disturbed dendritic arborization of PCs (panel G). MAPC therapy significantly prevented the increase of EGL/ML-ratio and loss of calbindin⁺ cells after global HI. HI and MAPC treatment did not induced changes in GFAP linear density. MAPC treatment significantly increased GFAP IR after global HI. Scale bar = 50 μm. EGL, external granular layer; GFAP, glial fibrillary acidic protein; HI, hypoxia-ischemia; IR, immunoreactivity; MAPC, multipotent adult progenitor cell; ML, molecular layer; PC, Purkinje cell; SAL, saline

cerebellum (Figure 3), indicating region-specific neuronal vulnerability in the cerebellum after global HI. Moreover, in the anterior lobe (Figure 3E) markedly more “gaps” within the PC layer were detected as compared to the posterior lobe (Figure 3G), indicating that loss of PCs was more pronounced in the anterior lobe. Caspase-3⁺ cells were moderately increased after global HI compared to controls, but the difference did not reach significance (sham-SAL vs HI-SAL $P = .100$).

Systemic MAPC administration prevented the alterations of cerebellar cortical strata after global HI as shown by a significantly decreased EGL/ML ratio in the total cerebellum (HI-SAL vs HI-MAPC $P = .021$). MAPC therapy prevented HI-induced loss of Purkinje cells as evidenced by significantly increased number of calbindin⁺ cells in the total cerebellum (HI-SAL vs HI-MAPC $P < .001$). Furthermore, the MAPCs prevented loss of dendritic arborization after global HI (Figure 2). No significant differences in EGL/ML ratio were found between the sham groups and the treatment group (HI-MAPC).

3.2 | Cortical Bergmann glia were not altered after global HI and MAPC therapy

We assessed linear fiber density of GFAP⁺ Bergmann glia, which are specialized astrocytes located in the ML of the cerebellar cortex and act as a migration scaffold for granule cells which in turn are important for PC development.^{24,25} Fiber linear density was not significantly altered following global HI (sham-SAL vs HI-SAL $P = .346$) (Figure 2I-L). Systemic MAPC administration did not alter GFAP⁺ fiber linear

density in the cerebellar cortex following HI (HI-SAL vs HI-MAPC $P = .559$) (Figure 2I-L).

No significant differences in GFAP IR were found in the cerebellar white matter (CTR vs HI $P = .999$) and cerebellar cortex GFAP IR (CTR vs HI $P = .999$) after global HI. MAPC administration significantly increased GFAP IR in the cerebellar cortex following HI (HI vs HI-MAPC $P = .017$) (Figure 2I-L). MAPCs did not alter GFAP expression in sham conditions.

3.3 | MAPC therapy region-specifically prevented histopathological cerebellar white matter injury after global HI

White matter injury was assessed by measuring area fraction of MBP IR and quantitative analysis of LFB staining. Global HI significantly reduced MBP IR in the cerebellar white matter (sham-SAL vs HI-SAL $P = .009$) indicating hypomyelination (Figure 4A-D). Both MBP (Figure 4B-D) and LFB (Figure 4F-H) staining showed evident disruption and disorganization of myelin sheaths in cerebellar white matter following global HI. No cystic formation or hemorrhages were found in all experimental groups in the cerebellum following global HI.

Systemic MAPC administration increased MBP-IR following global HI in the white matter of the cerebellum; however, the difference did not reach significance (HI-SAL vs HI-MAPC $P = .059$) (Figure 4A). Subanalysis indicated that MAPC administration did significantly increase MBP-IR in the posterior lobe of the cerebellum

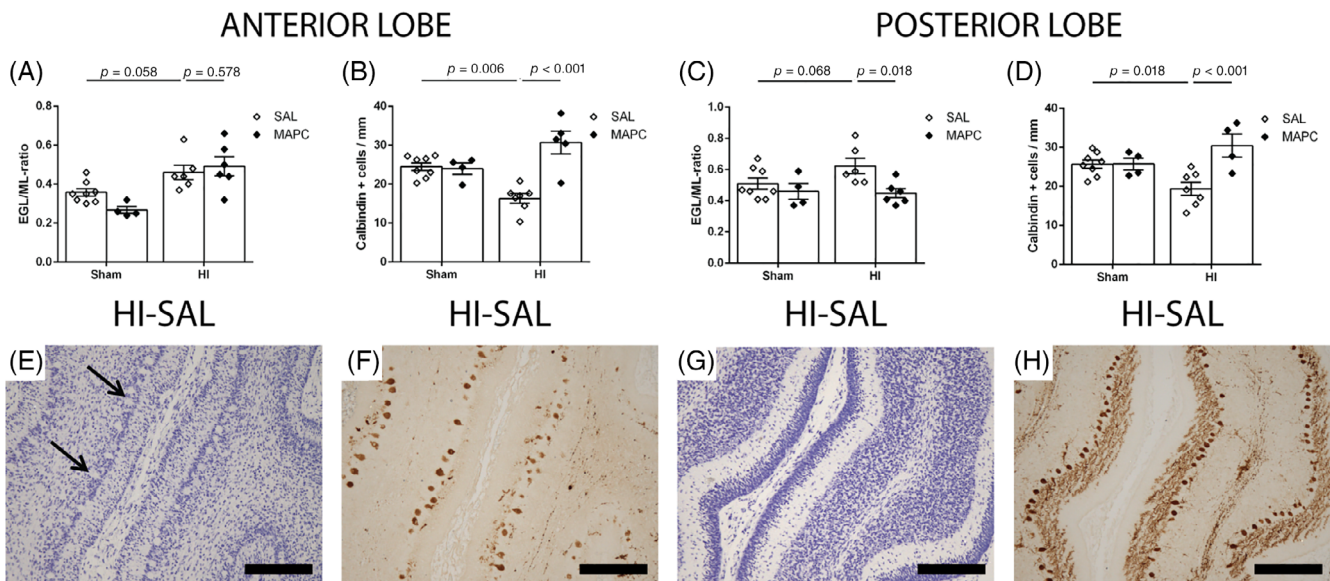


FIGURE 3 The anterior cerebellum displayed a morphological phenotype distinctly different from the posterior cerebellum following HI. A-D, Graphical presentation of EGL/ML-ratio and calbindin⁺ cells in the (A, B) anterior lobe and (C, D) posterior lobe. Means \pm SEM and levels of significance are depicted. E-H, Immunohistochemical (E, G) Nissl and (F, H) calbindin staining in the cerebellar cortex at $\times 100$ magnification. Global HI induced more pronounced disruption of cortical layers and loss of calbindin⁺ cells in the (E, F) anterior lobe compared to the (G, H) posterior lobe of the cerebellum. More “gaps” (arrows in panel E) within the PC layer of the anterior lobe were seen as compared to the posterior lobe. MAPC therapy prevented HI-induced calbindin⁺ cell loss in both lobes and prevented disruption of cortical strata in the posterior lobe. Scale bar = 200 μ m. EGL, external granular layer; HI, hypoxia-ischemia; MAPC, multipotent adult progenitor cell; ML, molecular layer; PC, Purkinje cell; SAL, saline

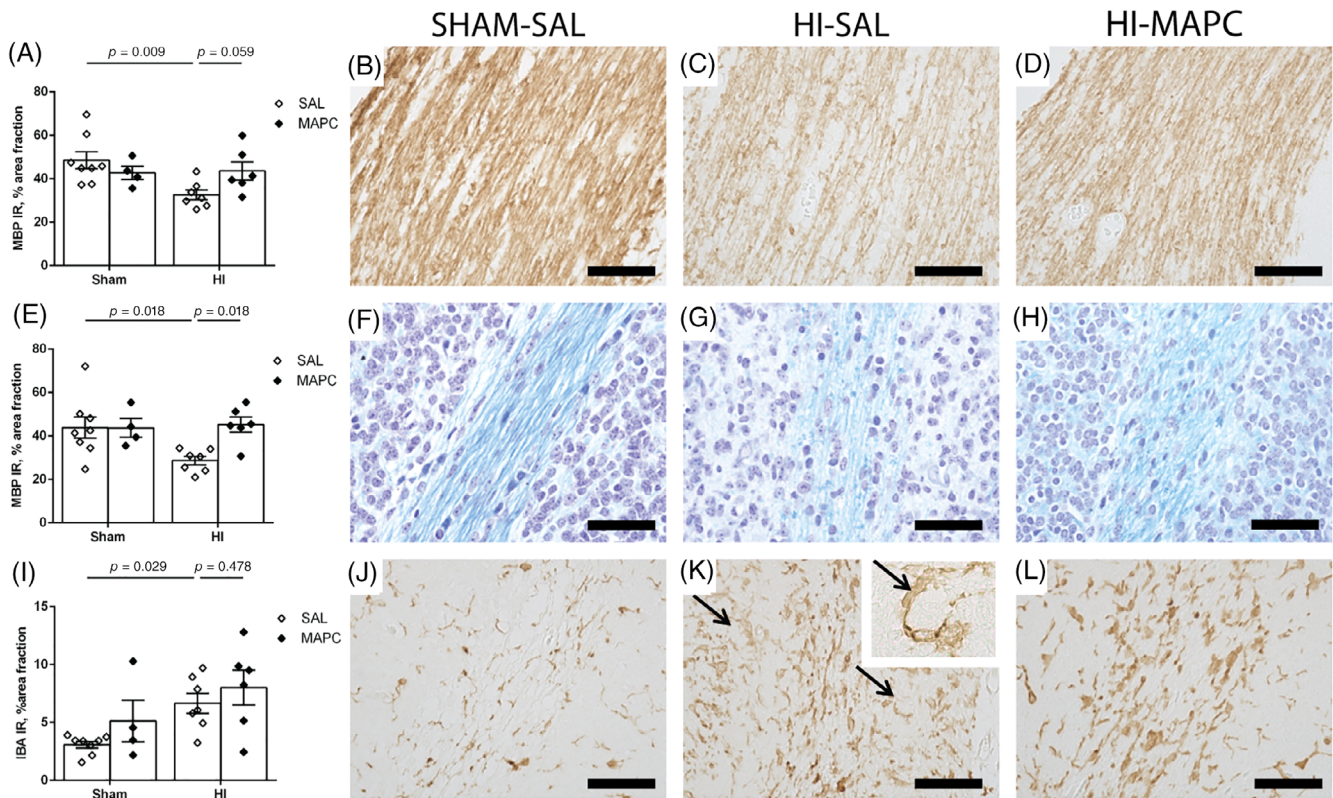


FIGURE 4 MAPC treatment region-specifically prevented disruption of white matter and hypomyelination without modulating microgliosis in the cerebellar white matter. Graphical presentation of (A, E) MBP IR area fractions of the (A) total cerebellum and (E) posterior lobes and (I) IBA-1 IR area fractions in the total cerebellar white matter. Means \pm SEM and levels of significance are depicted. Immunohistochemical (B-D) MBP, (F-H) Luxol fast blue, and (J-L) IBA-1 staining in the cerebellar white matter. Global HI caused marked hypomyelination with disorganization of myelin sheets and microglial proliferation in cerebellar white matter. Activated microglia were colocalized with PCs or “gaps” in the PC layer (arrows in insert of panel K). MAPC therapy prevented white matter injury in the preterm cerebellum after global HI. MAPC therapy did not alter microglial proliferation in cerebellar white matter. Images are taken at $\times 400$ magnification. Scale bar = 50 μ m. HI, hypoxia-ischemia; IR, immunoreactivity; MAPC, multipotent adult progenitor cell; MBP, myelin basic protein; PCs, Purkinje cells; SAL, saline

after global HI (HI-SAL vs HI-MAPC $P = .018$) (Figure 4E). No significant differences in MBP IR were detected between the sham groups and the treatment group (HI-MAPC).

3.4 | MAPC therapy did not alter histopathological microgliosis in the preterm cerebellum after global HI

The cerebellar inflammatory response after global HI was studied by assessing microglial proliferation using ionized calcium binding adaptor, which is a highly specific marker for resting and activated microglia in sheep.¹¹ Global HI significantly increased IBA-1 immunoreactivity in cerebellar white matter (sham-SAL vs HI-SAL $P = .029$) indicating microglial proliferation in this region (Figure 4H-K). Within the cerebellar white matter, IBA-IR was increased in the anterior lobes (sham-SAL vs HI-SAL $P = .018$) but did not reach significance in the posterior lobes (sham-SAL vs HI-SAL $P = .116$). In the cerebellar cortex, no significant change in IBA-1 IR was detected after global HI (sham-SAL vs HI-SAL $P = .073$) (data not shown). Morphological assessment showed that activated microglia were localized in close association with PCs following HI (Figure 4K, inset).

Systemic MAPC administration did not alter IBA-1 IR (HI-SAL vs HI-MAPC $P = .478$) in the preterm cerebellum following HI (Figure 4). No significant differences in IBA-1 IR were detected between the sham groups and the treatment group (HI-MAPC).

3.5 | MAPC therapy prevented microstructural changes detected by DTI in the cerebellar cortex after global HI

FA is a sensitive DTI marker to detect microstructural changes in both white matter and cortex.²⁶ FA values in the total cerebellum were significantly decreased following global HI (sham-SAL vs HI-SAL $P = .018$) (Figure 5). The decrease of FA values was particularly pronounced in the cerebellar cortex (sham-SAL vs HI-SAL $P = .009$) and did not reach statistical significance in cerebellar white matter (sham-SAL vs HI-SAL $P = .061$). In the cerebellar cortex, FA values were positively related to the number of calbindin⁺ cells in total cortex (Pearson's $r = 0.58$, $P = .018$) and in the posterior lobe (Pearson's $r = 0.66$, $P = .009$). FA values in cerebellar white matter were

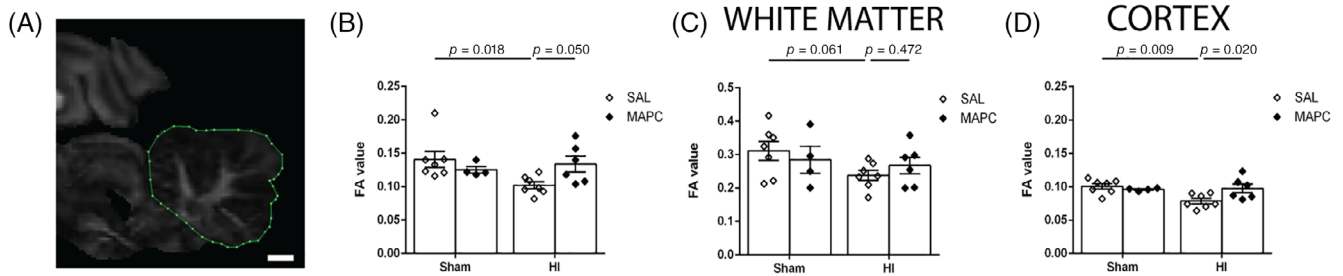


FIGURE 5 Microstructural changes detected by DTI in the preterm cerebellum following HI and MAPC treatment. A, Representative FA map depicting the delineation of the cerebellar region of interest. B-D, Graphical presentation of FA values in the (B) total cerebellum, (C) cerebellar white matter, and (D) cerebellar cortex. Means \pm 95% CI and levels of significance are depicted. Global HI significantly decreased FA values in the cerebellum, indicating disruption of cerebellar microstructure. MAPC therapy significantly protected the cerebellum against microstructural alterations, particularly in the cerebellar cortex. Scale bar = 5 mm. DTI, diffusion tensor imaging; FA, fractional anisotropy; HI, hypoxia-ischemia; MAPC, multipotent adult progenitor cell; SAL, saline

positively related to MBP IR in the total (Pearson's $r = 0.62$, $P = .002$) and anterior lobe of the cerebellum (Pearson's $r = 0.69$, $P < .001$).

Systemic MAPC administration significantly increased FA values of the total cerebellum (HI-SAL vs HI-MAPC $P = .050$). The MAPC-induced increase of FA values was particularly pronounced in cerebellar cortex (HI-SAL vs HI-MAPC $P = .020$) and did not reach statistical difference in cerebellar white matter (HI-SAL vs HI-MAPC $P = .472$) (Figure 5). No significant differences in FA values were detected between the sham groups and the treatment group (HI-MAPC).

4 | DISCUSSION

Cerebellar injury is increasingly recognized as a contributor to HIE in preterm infants. Nowadays, cell-based therapy is considered a promising strategy for the treatment of HI-induced white matter injury in the neonatal brain.²⁷ This is the first study in a preclinical large animal model demonstrating that systemic stem cell therapy may additionally have the potential to protect the preterm cerebellum after global HI.

We found in our model that global HI induced a pattern of injury with disrupted cortical strata, white matter injury and microgliosis in the preterm ovine cerebellum. More precisely, we showed that global HI increased the EGL/ML-ratio, which could not be explained by altered apoptotic cell death within this layer. The latter finding might be explained by the involvement of other mechanisms of cell death (ie, necrosis or autophagy) and/or timing of analysis, since apoptotic markers increased earlier (48 hours) after global HI in a similar fetal sheep model.²⁸ The altered EGL/ML ratio may also be the result of impeded migration of the granular cells from the EGL to the IGL reflecting cerebellar underdevelopment following global HI.² In line, global HI increased the number of ectopic PCs, which is indicative for a migration arrest of PCs from the ependymal zone to the cerebellar cortex.⁵ The disruption of cortical strata within this important developmental period may form the prestage for cerebellar underdevelopment which is frequently observed in preterm infants and associated with various neurodevelopmental disorders in later life.² The alterations in the cerebellar strata following global HI were paralleled by marked loss and reduced dendritic arborization of Purkinje cells

(PC) which play a pivotal role in structural and functional organization of cerebellar circuitry.^{29,30} Developmental disturbances in the cerebellar cortex were more pronounced in the anterior lobe as compared to the posterior lobe after global HI. This spatial vulnerability might reflect distinct molecular properties acquired during development rendering the anterior lobe more vulnerable to injury.^{31,32} We observed hypomyelination and disorganization of myelin structure in the preterm cerebellum following global HI, which in this model similarly occurred in the cerebral subcortical white matter as previously reported.¹¹ Excessive activation of microglia is considered as one of the essential steps leading to white matter injury.³³ Accordingly, we found increased microgliosis in the white matter of the cerebellum following global HI. Our findings are in line with previous studies demonstrating white matter injury in the ovine cerebellum after repeated global HI³⁴ or an alternative pro-inflammatory stimulus such as systemic endotoxin³⁵ indicating the vulnerability of cerebellar white matter during early development.

We demonstrated that early systemic MAPC treatment modulated the pattern of injury in the preterm cerebellum after global HI, as indicated by protection of ultrastructure of cortical strata, prevention of PC loss and region-specific prevention of cerebellar white matter injury. These findings extend our previous results showing that the MAPCs prevented hypomyelination of the periventricular white matter in the ovine preterm brain after global HI.¹¹

MAPCs have been shown to possess strong anti-inflammatory and regenerative properties.^{17,18} Therefore, the first dose of MAPCs was administered early after HI, targeted to modulate the emerging inflammatory response, which plays an important role in the etiology of HIE.³³ The second dose of MAPCs was administered in the subacute phase after global HI to support neuroregeneration after primary cell death has been initiated.³³ We showed that MAPCs prevented hypomyelination and reduced PC cell injury to control levels after global HI. We consider it to be unlikely that regeneration of PC cells and oligodendrocytes (and remyelination) would occur in the short follow-up period of 7 days. Therefore, we consider that neuroprotection was primarily established by the first dose of MAPCs by reducing direct cellular injury and dampening the peripheral and cerebral inflammatory response, rather than regeneration of

oligodendrocytes and PC cells by the second dose. Such pharmacological benefit of MAPC-driven immunomodulation was previously shown in experimental studies where MAPCs modulated the cerebral and peripheral inflammatory response after various types of central nervous system (CNS) injury, thereby providing an environment for recovery and repair of brain function and structure.^{17,18} More precisely, the neuroprotective effect was attributed to modulation of the peripheral inflammatory response in a spleen-mediated fashion^{18,36} and modulation of the cerebral inflammatory response by inducing a microglial-type switch from a pro-inflammatory M1 phenotype to an anti-inflammatory M2 phenotype.^{17,18,37} Despite protection of structure and cellularity of the cerebellar cortex and white matter, the current study did not confirm the hypothesis of MAPC-mediated modulation of microgliosis in the cerebellum. We postulate that this discrepancy could be explained by the fact that microgliosis in the cerebellum appeared to be milder than in the periventricular white matter¹¹ and that dynamics of white matter injury and repair in these two regions may differ. Furthermore, we could not confirm a MAPC-induced switch toward a dominant neuroprotective M2 phenotype since ovine-specific reagents are currently not available to discriminate M1 from M2 microglia. Moreover, we were not able to incorporate various time points to assess the cerebral inflammatory and structural changes over time or to discriminate between the therapeutic effect of the first and second dose of MAPCs. These limitations are inherent to limited experimental groups to make large animal experiments feasible. An alternative pathway by which MAPC therapy prevented neuronal loss might be by modification of astrocyte reactivity. GFAP⁺ astrocytes, including Bergmann glia, support injured neurons by the release of neurotrophic factors and nitric oxide synthase.⁵ Therefore, the increase in GFAP⁺ astrocyte activation after MAPC treatment in HI conditions might provide indirect support for PCs and account for the protection of these cells.

We showed neuroprotection with an early treatment strategy, which was initiated 1 hour after global HI. Recent work in a similar ovine model of HIE indicated that later (12-24 hours after global HI) administration of stem cells similarly protected the preterm brain.^{38,39} Moreover, recent clinical data showed that MAPCs are neuroprotective when administered 18 to 36 hours after ischemic stroke.¹⁴ Based on these combined findings, we expect that administration of MAPCs to neonates at a clinically more feasible time point (24 hours) after the hypoxic-ischemic event will result in comparable neuroprotective effects as shown in our current study.

The work in this preclinical animal model enabled us to correlate microstructural histological changes with DTI. Although acute cerebellar injury was found in a large (>80%) percentage of infants in human postmortem studies,⁴⁰ conventional MRI (eg, T1- and T2-weighted imaging) is notoriously poor in detecting acute cerebellar injury.⁴¹ We showed that DTI readily detected HI-induced injury and MAPC-mediated microstructural improvement, both of which were concurrently demonstrated with histopathology. Furthermore, FA values correlated well with several relevant histopathological markers of cerebellar injury, further indicating the added value of assessing microstructural injury and repair with this advanced imaging

technique. Our data suggest that DTI allows early detection of cerebellar alterations in pediatric patients. Therefore, we advocate the use of DTI to evaluate HI damage to the brain and to monitor the effects of future neuroprotective strategies in vivo in humans. However, not all histological changes in our study were detected by DTI and effect sizes appear to be more pronounced in histopathological analysis suggesting that even with advanced MRI techniques such as DTI, certain pathological phenomena could be underestimated. Currently, advanced imaging algorithms and postprocessing methods are being developed, which will increase sensitivity and specificity of DTI and thereby further improve the clinical use of DTI as a biomarker of individual neurodevelopment and therapeutic effect in the future.

One important limitation of this large animal study is the low number of animals. The dropout of one animal in the HI-MAPC group may have influenced therapeutic effect sizes. Given the relatively small animal numbers per group, we reported actual *P* values and tended to interpret *P* values between .05 and .1 as biologically relevant.⁴² This assumption decreases the chance of a false-negative finding but increases the chance that one of these differences is a false-positive result.⁴³ Importantly, the observed treatment effects in the cerebellum were consistent with our previous experimental work showing MAPC-mediated neuroprotection after global HI.¹¹

MAPCs have been approved for clinical use in adult CNS injury. A recent clinical trial in adult stroke patients showed that early administration of a single dose of MultiStem (the clinical name for the MAPC derived product) was safe and significantly improved functional outcomes after 1-year follow-up.¹⁴ An international multicentered phase III trial further evaluating the neuroprotective potential of these cells in adult stroke patients has been initiated in 2018 (ClinicalTrials.gov NCT03545607). Altogether, our findings of neuroprotection in the preterm cerebrum¹¹ and cerebellum may extend future clinical application of clinical-grade MAPCs from adult stroke to neonatal brain injury.

In conclusion, this is the first study in a preclinical animal model that indicated that early systemic MAPC therapy induced microstructural improvement in the preterm cerebellum following global HI. Moreover, microstructural alterations in the cerebellum were detectable with DTI, indicating the added clinical value of this imaging technique. Our findings underline the potential of MAPC therapy for the treatment of preterm brain injury after HI.

ACKNOWLEDGMENTS

The authors would like to thank Lilian Kessels for technical support and Freek Hoebeek for proofreading the manuscript. Athersys, Inc., sponsored this study, and its affiliate ReGenesys BVBA provided MAPCs. Athersys, Inc., and ReGenesys BVBA were not involved in the experimental design, statistical analysis, data presentation, or decision to publish.

CONFLICT OF INTEREST

R.W.M. declared employment with Athersys, Inc., the company providing the cells in this study. The other authors declared no potential conflicts of interest.

AUTHOR CONTRIBUTIONS

R.G., D.R.M.G.O.: collection and/or assembly of data, data analysis and interpretation, manuscript writing, final approval of manuscript; J.D., K.P.: data analysis and interpretation, manuscript writing, final approval of manuscript; M.L.: data analysis and interpretation, final approval of manuscript; R.W.M.: provision of study material or patients, financial support, final approval of manuscript; L.J.Z.: conception and design, final approval of manuscript; B.W.K.: conception and design, manuscript writing, final approval of manuscript; T.G.A.M.W.: conception and design, data analysis and interpretation, manuscript writing, final approval of manuscript; R.K.J.: conception and design, collection and/or assembly of data, data analysis and interpretation, manuscript writing, final approval of manuscript.

DATA AVAILABILITY STATEMENT

The data that support the findings of this study are available from the corresponding author upon reasonable request.

ORCID

Tim G.A.M. Wolfs  <https://orcid.org/0000-0003-4417-4144>

Reint K. Jellema  <https://orcid.org/0000-0002-6918-0930>

REFERENCES

- Volpe JJ. Brain injury in premature infants: a complex amalgam of destructive and developmental disturbances. *Lancet Neurol.* 2009;8:110-124.
- Volpe JJ. Cerebellum of the premature infant: rapidly developing, vulnerable, clinically important. *J Child Neurol.* 2009;24:1085-1104.
- Stoodley CJ, Limperopoulos C. Structure-function relationships in the developing cerebellum: evidence from early-life cerebellar injury and neurodevelopmental disorders. *Semin Fetal Neonatal Med.* 2016;21:356-364.
- Hammerl M, Zagler M, Griesmaier E, et al. Reduced cerebellar size at term-equivalent age is related to a 17% lower mental developmental index in very preterm infants without brain injury. *Neonatology.* 2020;117:57-64.
- Hutton LC, Yan E, Yawno T, Castillo-Melendez M, Hirst JJ, Walker DW. Injury of the developing cerebellum: a brief review of the effects of endotoxin and asphyxial challenges in the late gestation sheep fetus. *Cerebellum.* 2014;13:777-786.
- Kwan S, Boudes E, Gilbert G, et al. Injury to the cerebellum in term asphyxiated newborns treated with hypothermia. *AJNR Am J Neuroradiol.* 2015;36:1542-1549.
- Johnsen SD, Bodensteiner JB, Lotze TE. Frequency and nature of cerebellar injury in the extremely premature survivor with cerebral palsy. *J Child Neurol.* 2005;20:60-64.
- Pieterman K, White TJ, van den Bosch GE, et al. Cerebellar growth impairment characterizes school-aged children born preterm without perinatal brain lesions. *AJNR Am J Neuroradiol.* 2018;39:956-962.
- Bennet L, Tan S, Van den Heuvel L, et al. Cell therapy for neonatal hypoxia-ischemia and cerebral palsy. *Ann Neurol.* 2012;71:589-600.
- Jellema RK, Wolfs TG, Lima Passos V, et al. Mesenchymal stem cells induce T-cell tolerance and protect the preterm brain after global hypoxia-ischemia. *PLoS One.* 2013;8:e73031.
- Jellema RK, Ophelders DR, Zwanenburg A, et al. Multipotent adult progenitor cells for hypoxic-ischemic injury in the preterm brain. *J Neuroinflammation.* 2015;12:241.
- Boozer S, Lehman N, Lakshminpathy U, et al. Global characterization and genomic stability of human MultiStem, a multipotent adult progenitor cell. *J Stem Cells.* 2009;4:17-28.
- Kovacsovics-Bankowski M, Mauch K, Raber A, et al. Pre-clinical safety testing supporting clinical use of allogeneic multipotent adult progenitor cells. *Cytotherapy.* 2008;10:730-742.
- Hess DC, Wechsler LR, Clark WM, et al. Safety and efficacy of multipotent adult progenitor cells in acute ischaemic stroke (MASTERS): a randomised, double-blind, placebo-controlled, phase 2 trial. *Lancet Neurol.* 2017;16:360-368.
- Cunha JP, Leuckx G, Sterkendries P, et al. Human multipotent adult progenitor cells enhance islet function and revascularisation when co-transplanted as a composite pellet in a mouse model of diabetes. *Diabetologia.* 2017;60:134-142.
- Mays RW, Borlongan CV, Yasuhara T, et al. Development of an allogeneic adherent stem cell therapy for treatment of ischemic stroke. *J Exp Stroke Transl Med.* 2010;3:34-46.
- Busch SA, Hamilton JA, Horn KP, et al. Multipotent adult progenitor cells prevent macrophage-mediated axonal dieback and promote regrowth after spinal cord injury. *J Neurosci.* 2011;31:944-953.
- DePaul MA, Palmer M, Lang BT, et al. Intravenous multipotent adult progenitor cell treatment decreases inflammation leading to functional recovery following spinal cord injury. *Sci Rep.* 2015;5:16795.
- Back SA, Riddle A, Hohimer AR. Role of instrumented fetal sheep preparations in defining the pathogenesis of human periventricular white-matter injury. *J Child Neurol.* 2006;21:582-589.
- Leemans A, Jones DK. The B-matrix must be rotated when correcting for subject motion in DTI data. *Magn Reson Med.* 2009;61:1336-1349.
- Irfanoglu MO, Walker L, Sarlls J, Marengo S, Pierpaoli C. Effects of image distortions originating from susceptibility variations and concomitant fields on diffusion MRI tractography results. *Neuroimage.* 2012;61:275-288.
- Tax CM, Otte WM, Viergever MA, et al. REKINDLE: robust extraction of kurtosis INDices with linear estimation. *Magn Reson Med.* 2015;73:794-808.
- Ophelders DR, Wolfs TG, Jellema RK, et al. Mesenchymal stromal cell-derived extracellular vesicles protect the fetal brain after hypoxia-ischemia. *STEM CELLS TRANSLATIONAL MEDICINE.* 2016;5:754-763.
- Lordkipanidze T, Dunaevsky A. Purkinje cell dendrites grow in alignment with Bergmann glia. *Glia.* 2005;51:229-234.
- Tolcos M, McDougall A, Shields A, et al. Intrauterine growth restriction affects cerebellar granule cells in the developing Guinea pig brain. *Dev Neurosci.* 2018;40:162-174.
- Alexander AL, Lee JE, Lazar M, Field AS. Diffusion tensor imaging of the brain. *Neurotherapeutics.* 2007;4:316-329.
- Gortner L, Felderhoff-Muser U, Monz D, et al. Regenerative therapies in neonatology: clinical perspectives. *Klin Padiatr.* 2012;224:233-240.
- Hutton LC, Castillo-Melendez M, Walker DW. Uteroplacental inflammation results in blood brain barrier breakdown, increased activated caspase 3 and lipid peroxidation in the late gestation ovine fetal cerebellum. *Dev Neurosci.* 2007;29:341-354.
- Daskalakis ZJ, Paradiso GO, Christensen BK, Fitzgerald PB, Gunraj C, Chen R. Exploring the connectivity between the cerebellum and motor cortex in humans. *J Physiol.* 2004;557:689-700.
- Akkal D, Dum RP, Strick PL. Supplementary motor area and presupplementary motor area: targets of basal ganglia and cerebellar output. *J Neurosci.* 2007;27:10659-10673.
- Cerminara NL, Lang EJ, Sillitoe RV, Apps R. Redefining the cerebellar cortex as an assembly of non-uniform Purkinje cell microcircuits. *Nat Rev Neurosci.* 2015;16:79-93.
- D'Mello AM, Stoodley CJ. Cerebro-cerebellar circuits in autism spectrum disorder. *Front Neurosci.* 2015;9:408.
- Hagberg H, Mallard C, Ferriero DM, et al. The role of inflammation in perinatal brain injury. *Nat Rev Neurol.* 2015;11:192-208.

34. Castillo-Melendez M, Chow JA, Walker DW. Lipid peroxidation, caspase-3 immunoreactivity, and pyknosis in late-gestation fetal sheep brain after umbilical cord occlusion. *Pediatr Res.* 2004;55: 864-871.
35. Dean JM, Farrag D, Zahkook SA, et al. Cerebellar white matter injury following systemic endotoxemia in preterm fetal sheep. *Neuroscience.* 2009;160:606-615.
36. Walker PA, Shah SK, Jimenez F, et al. Intravenous multipotent adult progenitor cell therapy for traumatic brain injury: preserving the blood brain barrier via an interaction with splenocytes. *Exp Neurol.* 2010;225:341-352.
37. Walker PA, Bedi S, Shah SK, et al. Intravenous multipotent adult progenitor cell therapy after traumatic brain injury: modulation of the resident microglia population. *J Neuroinflammation.* 2012; 9:228.
38. Li J, Yawno T, Sutherland A, et al. Preterm white matter brain injury is prevented by early administration of umbilical cord blood cells. *Exp Neurol.* 2016;283:179-187.
39. van den Heuvel LG, Fraser M, Miller SL, et al. Delayed intranasal infusion of human amnion epithelial cells improves white matter maturation after asphyxia in preterm fetal sheep. *J Cereb Blood Flow Metab.* 2019;39(2):223-239.
40. Alderliesten ME, Peringa J, van der Hulst VP, et al. Perinatal mortality: clinical value of postmortem magnetic resonance imaging compared with autopsy in routine obstetric practice. *BJOG.* 2003; 110:378-382.
41. Vermeulen RJ, Fetter WP, Hendriks L, van Schie P, van der Knaap M, Barkhof F. Diffusion-weighted MRI in severe neonatal hypoxic ischaemia: the white cerebrum. *Neuropediatrics.* 2003;34:72-76.
42. Wasserstein RL, Schirm AL, Lazar NA. Moving to a world beyond "p < 0.05". *Am Stat.* 2019;73:1-19.
43. Amrhein V, Greenland S, McShane B. Scientists rise up against statistical significance. *Nature.* 2019;567:305-307.

SUPPORTING INFORMATION

Additional supporting information may be found online in the Supporting Information section at the end of this article.

How to cite this article: Gussenhoven R, Ophelders DRMG, Dudink J, et al. Systemic multipotent adult progenitor cells protect the cerebellum after asphyxia in fetal sheep. *STEM CELLS Transl Med.* 2021;10:57-67. <https://doi.org/10.1002/sctm.19-0157>